Oikos

OIK-06146

Pirotta, E., Mangel, M., Costa, D. P., Goldbogen, J., Harwood, J., Hin, V., Irvine, L. M., Mate, B. R., McHuron, E. A., Palacios, D. M., Schwarz, L. K. and New, L. 2019. Anthropogenic disturbance in a changing environment: modelling lifetime reproductive success to predict the consequences of multiple stressors on a migratory population. – Oikos doi: 10.1111/oik.06146

Appendix 1

Modifications to the model for one reproductive cycle

Pirotta et al. (2018) assumed that modelled females were at their asymptotic length (22 m). In contrast, in this study we modelled a female's growth over her lifetime. As a result, all parameters that resulted from allometric relationships with body length or mass were calculated for each day in the life of a female (that is, for each length or lean mass value). These included all metabolic rates (e.g. rorqual average active metabolic rate (Potvin et al. 2012) and cost of transport (Williams 1999)), the size of the buccal cavity, the forestomach capacity, the maximum and minimum value of blubber mass a female could carry (although percentages of total mass remained fixed at the original 5% and 35% values) and the threshold blubber mass above which a lactating female delivered milk to her dependent calf (based on the same value of 16% used by Pirotta et al. 2018).

Because a calf needs to store proportionally more lipid reserves than an adult to grow, the upper range of the calf's proportion of blubber mass was 0.44, while an adult's maximum proportion was 0.35 (Pirotta et al. 2018). In order to reconcile this change in maximum storage abilities, we assumed a linear decline from 0.44 to 0.35 over the course of the juvenile years of a female (i.e. between 7 months and 6 years of age).

Pirotta et al. (2018) assumed a fixed metabolic rate for the suckling calf of 836.8 MJ/d (Lockyer 1981). Here, we modelled the variation of the calf's metabolic rate explicitly as a function of its growing size. Specifically, we used the same allometric relationship between basal metabolic rate and mass by Kleiber (1975), reported in Potvin et al. (2012).

In the original model, female blubber mass varied in increments of 500 kg for ease of derivation of the Stochastic Dynamic Programming equations. Increments of this size would have resulted in a number of bins for this state variable that caused the storage arrays over all combinations of state variables and all days in the lifetime of a female to exceed computer memory,

and the backward derivation to slow down to unfeasible run times (i.e., years to finish). Thus, we substituted this fixed size with an adaptive bin size. We relied on preliminary runs of the model that used a coarse bin size (2,000 kg) to explore the relationship between female blubber mass and fitness at different moments in time, and identified regions in the range of this state variable where finer bins were needed for an appropriate characterization of this relationship. As a result, our bins were at 500, 1,000, 1,500, 2,000, 2,500, 3,000, 3,500, 4,000, 4,700, 5,300, 6,000, 7,000, 8,000, 8,700, 9,300, 10,000, 11,000, 12,000, 14,000, 16,000, 18,000, 20,000 and 22,000 kg of female blubber mass. Similarly, we reduced the number of bins for the calf's proportion of blubber mass and used fixed increments of 0.03, which was deemed sufficient to represent the relationship between this state variable and fitness.

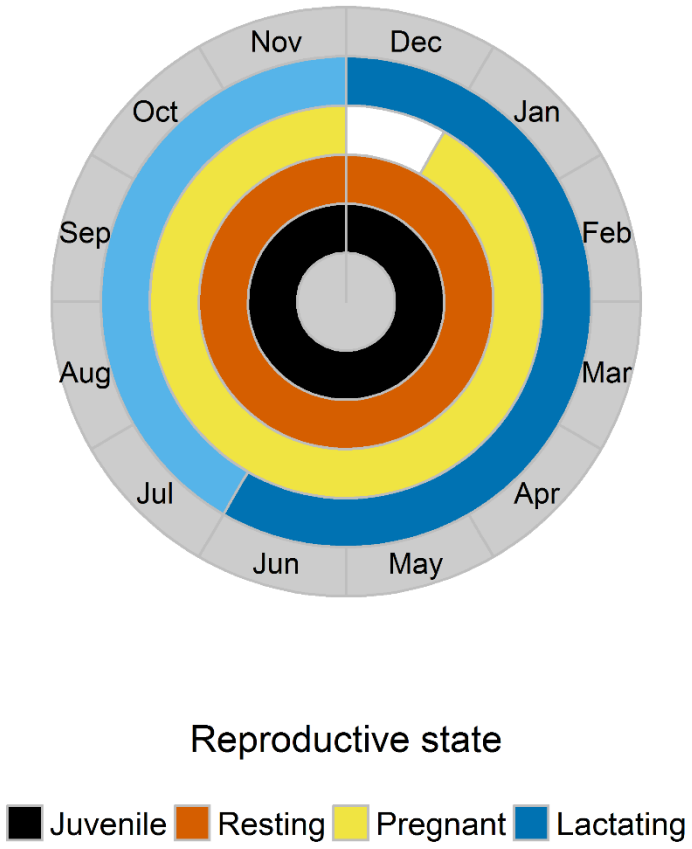

Figure A1. Potential reproductive state of a female blue whale at different times of the year. Implantation is assumed to occur on the 1 January and birth is assumed to occur on the 1 December. Resting indicates a female that is not pregnant nor lactating. The light blue area represents the possible extension of lactation beyond the seven-month threshold of autonomous feeding. The white area represents the time a female is not pregnant.

Appendix 2

Stochastic dynamic programming equations

A female's lifetime fitness is defined as the expected maximum accumulated calf survival (i.e. the calves that survive to become independent members of the population) taken over the stochasticity of mortality events and of the environment. Females increase lifetime fitness at each weaning event by adding a calf to the population with a probability that depends upon the proportion of a calf's mass that is blubber at 7 months or later, m, as defined by the terminal fitness function: $\varphi(m) = m^{\gamma} / (m^{\gamma} + m_{50}^{\gamma})$, where $m_{50} = 0.27$ and $\gamma = 8$ (Pirotta et al. 2018).

A female can be in one of four reproductive states (Supplementary material Fig. A1): juvenile (i.e. before reaching sexual maturity; 1); mature, not pregnant and not lactating (i.e, resting; 2); mature and pregnant (3); mature and lactating (i.e. with a dependent calf; 4). Given her blubber mass at time t, $X(t) = x$, the calf's proportion of blubber mass (if in state 4), $M(t) = m$, her location, $L(t) = l$, and the current patch type, $I(t) = i$, we denote the fitness functions for females in each state by $F_1(x,l,i,t)$, $F_2(x,l,i,t)$, $F_3(x,l,i,t)$, and $F_4(x,m,l,i,t)$, respectively. Age is taken to be $a = 0, 1, 2, \ldots, a_M - 1$ for juveniles, where $a_M = 6$ is the age of sexual maturity. For adults, $a = a_M + n$, where $n = 0, 1, 2, \ldots, N$; $N = 90$ is the duration of the reproductive life of a female, after which death occurs. While weaning can occur at any time during lactation, birth and implantation only occur on the 1st, $t_B = 1$, and 32nd, $t_I = 32$, day of each modelled year, respectively, i.e. for the n^{th} reproductive event:

$t_b(n) = t_B + (a_M + n) \cdot 365$

$t_i(n) = t_I + (a_M + n) \cdot 365$.

Below, we outline a female's fitness at different moments of her life, starting from the last reproductive year. We follow Pirotta et al. (2018) for details of the state dynamics given different behavioural choices. In all equations, the notation $\langle F_s \rangle$ is used to indicate the maximum expected value of the terminal fitness taken over all possible behavioural decisions (stay in the current location and feed, move forward, move backward, or move within the breeding locations), background levels of mortality and environmental stochasticity, given the current value of the state variables and reproductive state, s. For example, $F_2(x,l,i,t) = \langle F_2 \rangle = \max\{V_{2,b}(x,l,i,t)\}$, where $V_{2,b}(x,l,i,t)$ is the fitness value of behavioural choice b when in reproductive state 2 at time t.

- During the last year, $n = N$, a female can be in:

State 2 (mature, not pregnant, not lactating):

$F_2(x,l,i,t) = \langle F_2 \rangle$.

At $t = T - 1$: $F_2(x,l,i,T-1) = 0$.

State 4 (mature, not pregnant, lactating):

$F_4(x,m,l,i,t) = \max\{\langle F_4 \rangle, \varphi(m) + \langle F_2 \rangle\}$, i.e. she can either keep or wean the calf.

At $t = T - 1$: $F_4(x,m,l,i,T-1) = \varphi(m)$, i.e. she weans her last calf.

- In any other year of her reproductive life, $n \leq (N-1)$, a female can be in:

State 2 (mature, not pregnant, not lactating):

$F_2(x,l,i,t) = <F_2>$.

At $t = t_i(n)$: $F_2(x,l,i,t_i(n)) = \max\{<F_3>, <F_2>\}$, i.e. she can implant and become pregnant.

State 3 (mature, pregnant, not lactating):

$F_3(x,l,i,t) = \max\{<F_3>, <F_2>\}$, i.e. she can remain pregnant or abort the foetus.

At $t = t_b(n+1) - 1$: $F_3(x,l,i,t_b(n+1)-1) = \max\{<F_4>, <F_2>\}$, i.e. she can abort or give birth.

State 4 (mature, not pregnant, lactating):

$F_4(x,m,l,i,t) = \max\{<F_4>, \varphi(m) + <F_2>\}$, i.e. she can either keep or wean the calf.

At $t = t_b(n+1) - 1$: $F_4(x,m,l,i,t) = \varphi(m) + <F_2>$, i.e. she weans the calf.

- During her juvenile years, $a < a_M$, a female can be in:

State 1 (juvenile):

$F_1(x,l,i,t) = <F_1>$.

At $t = t_b(0) - 1$: $F_1(x,l,i,t_b(0)-1) = <F_2>$.

Appendix 3

Transition between environmental regimes

The equations presented in the previous section assume a unique set of stochastic environmental conditions. In order to capture blue whales' adaptation to periodic oscillations in their habitat, we modelled the transition between two environmental regimes, representing standard and unfavourable conditions. The shift between the two regimes could occur at the start of each calendar year ($t_E = 31$ in model time), i.e. for the a^{th} year of a whale's life:

$t_e(a) = t_E + a \cdot 365$

Given current reproductive state s and the current value of the state variables (x, l, i and, when lactating, m), then on any day $t \neq t_e(a)$:

$F_{g,s}(x,l,i,t) = \max\{V_{g,s,b}(x,l,i,t)\}$

and

$F_{u,s}(x,l,i,t) = \max\{V_{u,s,b}(x,l,i,t)\}$,

where g and u indicate the fitness value of behavioural choice b calculated under standard and unfavourable environmental conditions, respectively.

At $t = t_e(a)$, given the probability of a year being unfavourable, $p_u = 0.2$:

$F_{g,s}(x,l,i,t_e(a)) = \max\{(1 - p_u) \cdot V_{g,s,b}(x,l,i,t_e(a)) + p_u \cdot V_{u,s,b}(x,l,i,t_e(a))\}$

and

$F_{u,s}(x,l,i,t_e(a)) = \max\{p_u \cdot V_{u,s,b}(x,l,i,t_e(a)) + (1 - p_u) \cdot V_{g,s,b}(x,l,i,t_e(a))\}$.

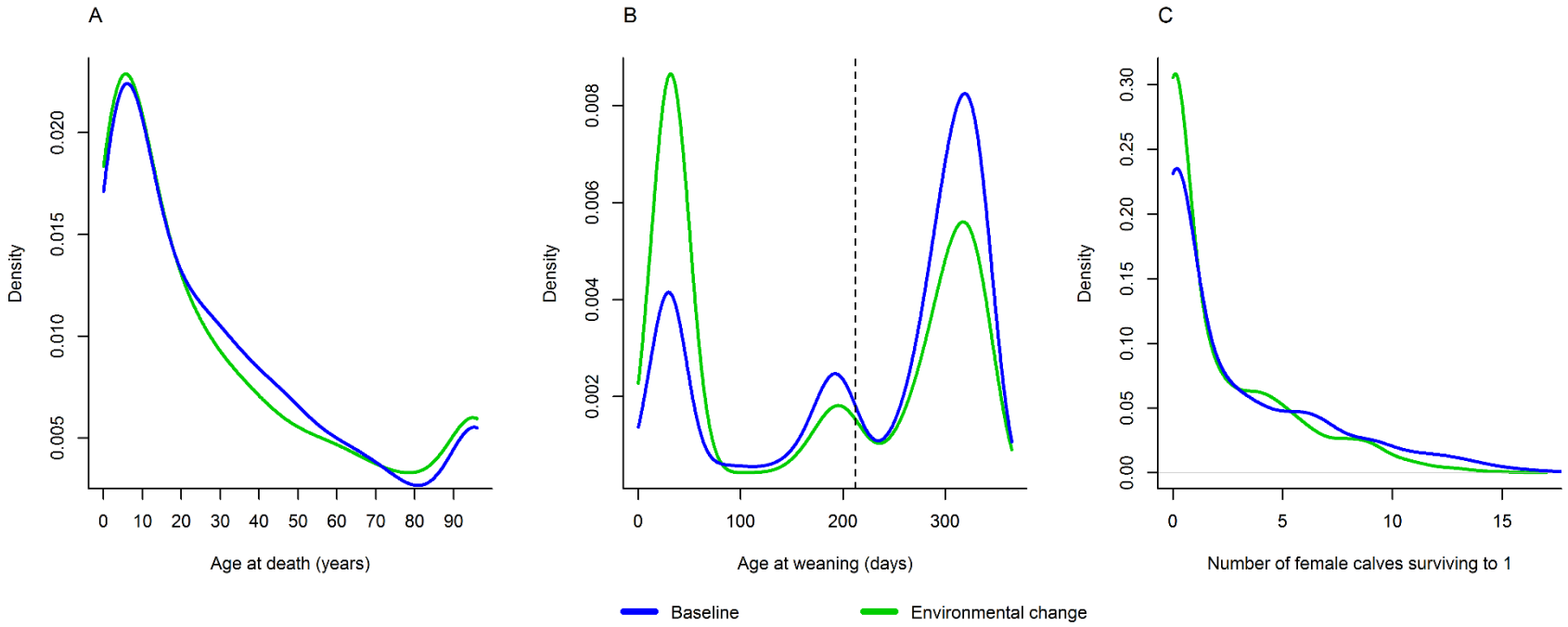

Figure A2. Example of results of simulated environmental change (scenario 2). Comparison of kernel probability densities of A) female survival; B) calf age at weaning (the vertical dashed line indicates the threshold for autonomous feeding, 7 months); and C) female reproductive success, under baseline (blue) and altered (green) conditions.

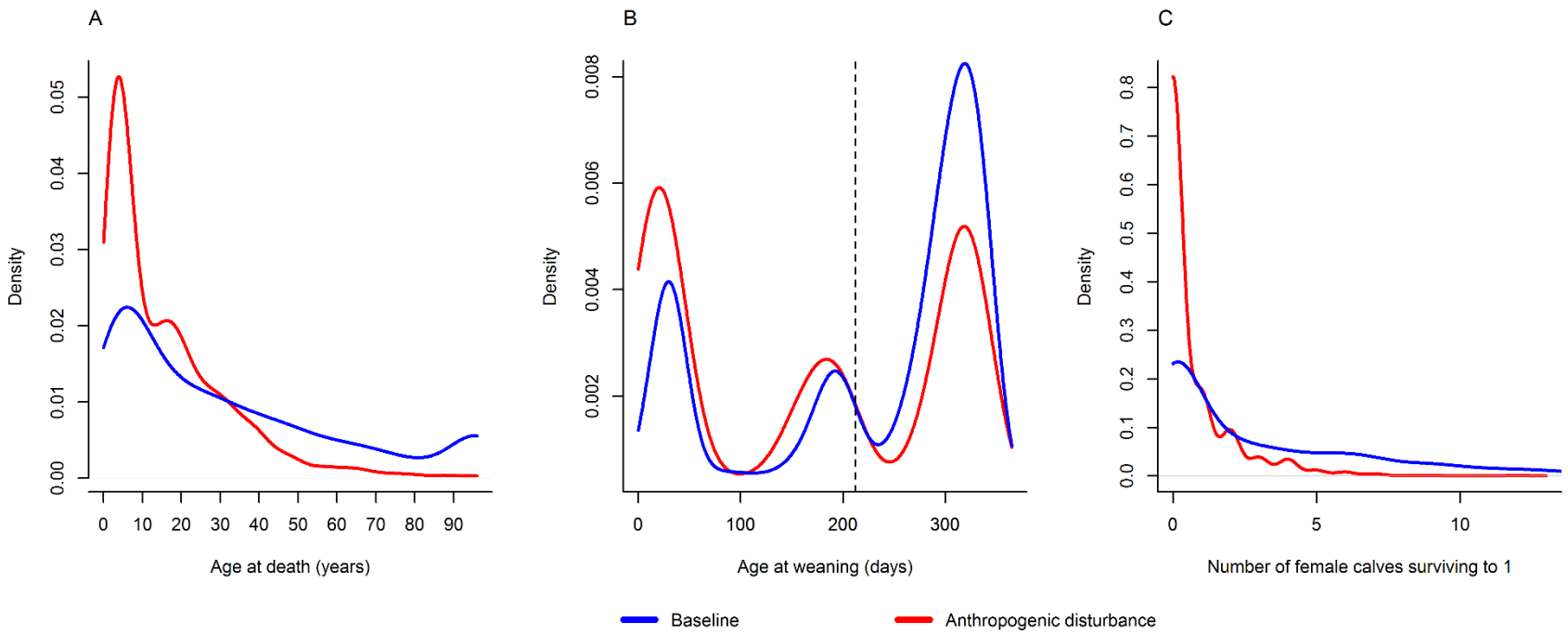

Figure A3. Example of results of simulated anthropogenic disturbance (scenario 32). Comparison of kernel probability densities of A) female survival; B) calf age at weaning (the vertical dashed line indicates the threshold for autonomous feeding, 7 months); and C) female reproductive success, under baseline (blue) and disturbed (red) conditions.

Appendix 4

Density dependence

Most wildlife populations cannot grow indefinitely because they live in environments that have finite resources. Carrying capacity is defined as the population size at which birth and death rates balance. When population size approaches carrying capacity, density-dependent processes are triggered, reducing a population's growth rate until it stabilises at 1. Density dependence is generally mediated by a reduction in the resources available to each individual due to competition, to which animals' behavioural and reproductive decisions are likely adapted. As a result, in a dynamic state variable model these effects should be part of the optimisation procedure and thus built in the backward iteration (Mangel and Clark 1988). This extension would require substantial model development that was beyond the scope of the present study. However, as a temporary alternative when simulating a population that is close to carrying capacity, a mechanism for density dependence can be introduced in the forward iteration in the form of a step function (Supplementary material Fig. A4). We demonstrate this potential extension of the model here. (Monnahan et al. 2015) estimated carrying capacity for eastern North Pacific blue whales to be $K = 2{,}210$ (95% confidence interval: 1,823–3,721). This corresponds to a mean female carry capacity $K_f = 1105$. We assumed that individuals would start to compete when population size reached $K_f - 50$; this value ensured that population size stabilised at K_f, and was obtained from preliminary simulations. Above this population size, each additional individual contributed to reduce the overall amount of resources by a factor $i_U = 1/(K_f - 50)$, representing the relative amount of resources available to each individual before the triggering of density-dependent processes. In the most extreme scenario, the amount of resources could be reduced to 0, which occurred at female population size equal to $2 \cdot K_f - 100$. We set the initial population size at 850 females to reflect the most recent abundance estimate for blue whales feeding in the California Current (Calambokidis and Barlow 2013). In the absence of information on the population's age structure, we drew the initial age, reproductive state, blubber mass and location of each simulated female from the distributions of these variables in a trial simulation at stability (excluding unfavourable years). We included unfavourable years with the same frequency as in the main simulations (1 every 5 years). The simulation was run for 100 years and repeated 25 times, in order to capture variability among simulations while retaining feasible run times.

Simulated populations rapidly reached carrying capacity; density dependence then caused population size to oscillate around this average value, consistent with the theorem of (Parsons 2018). The specific temporal dynamics of each simulated population varied stochastically with the relative timing between the onset of density-dependent processes and the occurrence of unfavourable years (Supplementary material Fig. A5): the effect of unfavourable environmental conditions could be amplified or attenuated depending on whether these occurred in conjunction with density-dependent competition with other individuals or on years where population size was below carrying capacity. Individual survival and reproductive success were both highly affected by density dependence. Females tended to die at a younger age due to increased starvation rate (Supplementary material Fig. A6). Cohen's *d* suggested the difference in survival between simulations with and without carrying capacity was large (mean across the 25 replicates = 0.78). As in the simulations without carrying capacity, juvenile individuals were the class mostly affected by death from starvation. In terms of reproduction, the mean inter-birth interval remained essentially unchanged (2.43 [2.41 – 2.45]), but the mean interval between calves surviving to age 1 y increased to 8.25 [7.76 – 8.79] and the mean number of female calves surviving to age 1 y per female dropped to 0.98 [0.95 – 1.04]. Cohen's *d* indicated that the difference in female lifetime reproductive success was intermediate to large (mean across the 25 replicates = 0.61).

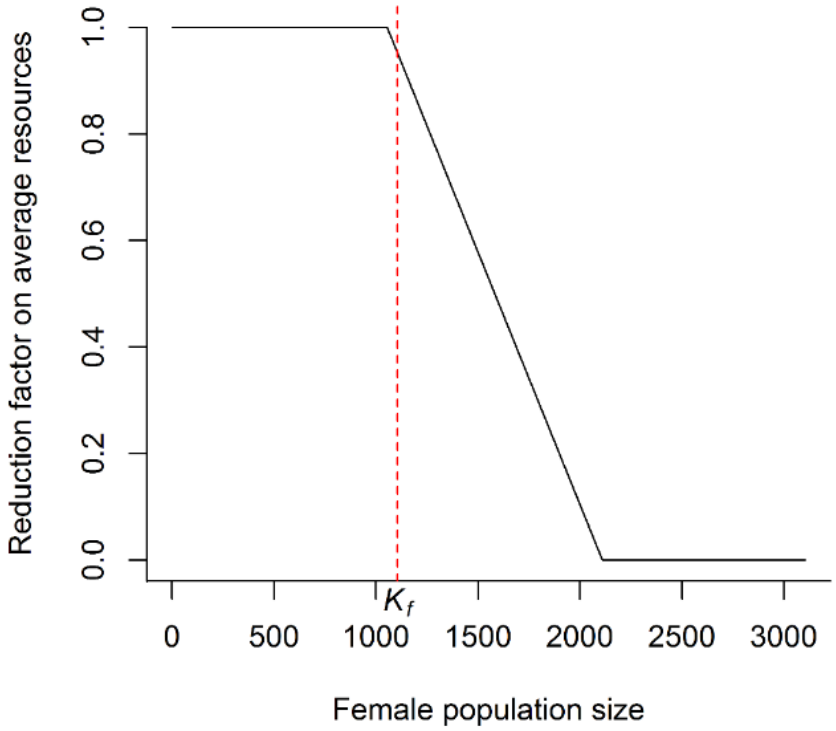

Figure A4. Step function representing the reduction factor on the average amount of resources for increasing female population size (i.e., a linear decrease over the range $K_f - 50$ to $2 \cdot K_f - 100$). The dashed red line indicates female carrying capacity, $K_f = 1{,}105$.

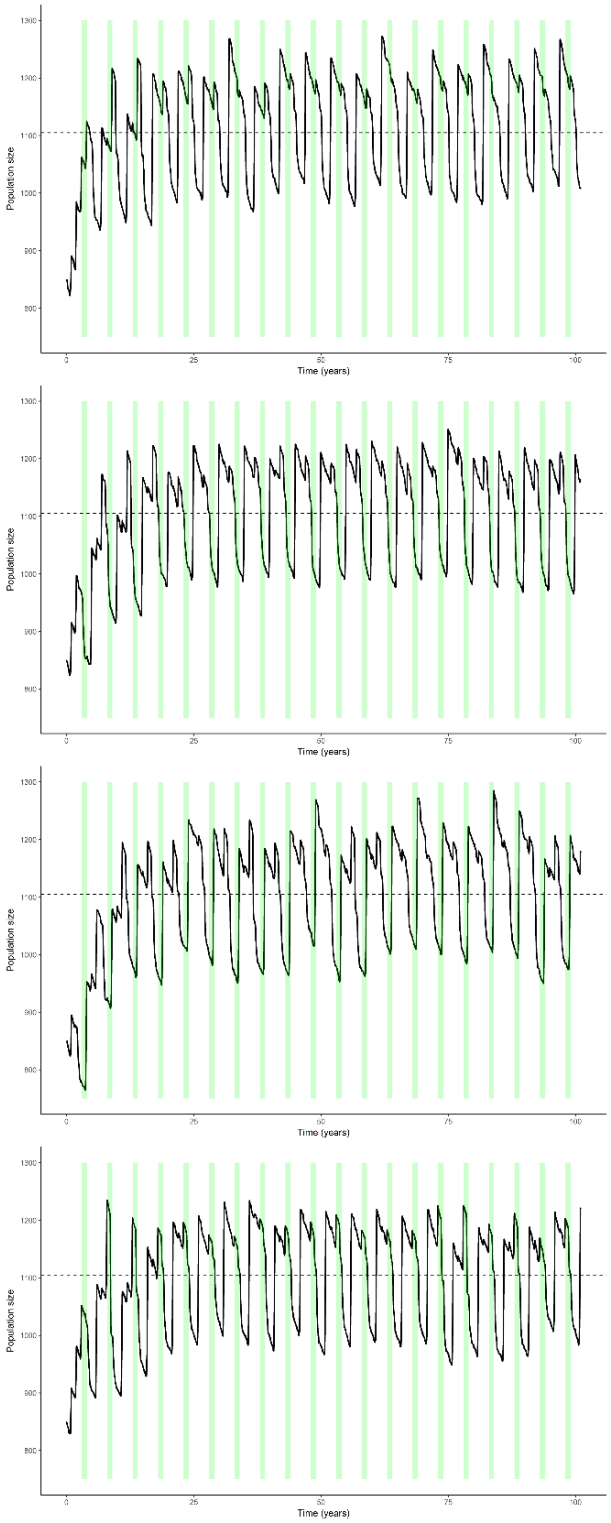

Figure A5. Temporal variation in population size for four sample runs of the forward simulation including the effects of density dependence. The green shaded areas represent unfavourable years. The dashed horizontal line indicates mean female carry capacity, $K_f = 1105$.

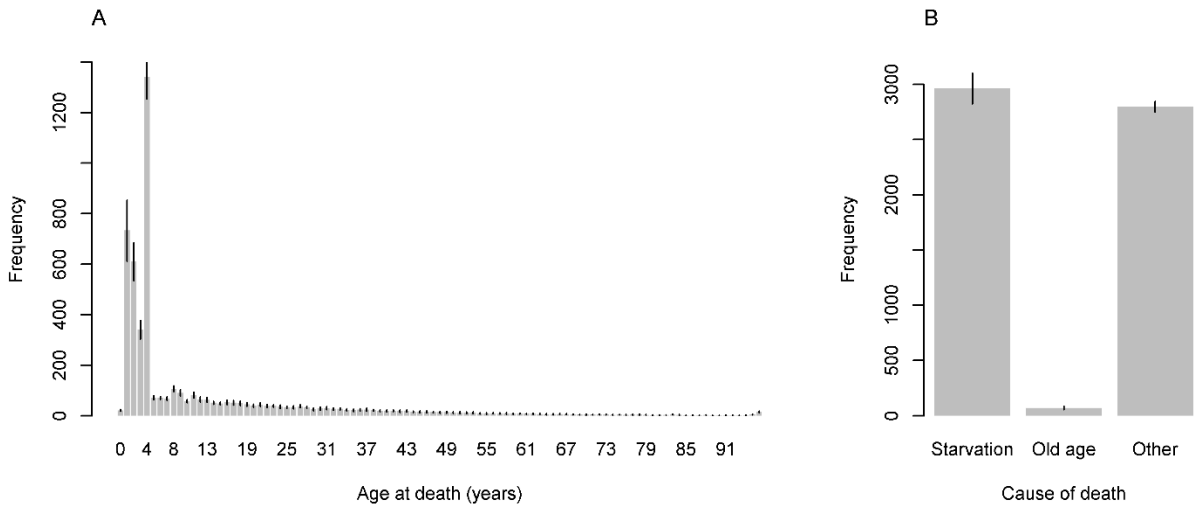

Figure A6. Survival patterns of simulated females under density dependence. In (A) distribution of age at death; in (B), bar plot of the causes of death. Black segments represent the standard deviation across the 25 runs of the simulation.

Appendix 5

Model code

The archive contains the R code, Rcpp functions and all associated files required to run the backward and forward iterations of the model in R (Eddelbuettel and Francois 2011, R Development Core Team 2016).

References

Calambokidis, J. and Barlow, J. 2013. Updated abundance estimates of blue and humpback whales off the US west coast incorporating photo-identifications from 2010 and 2011. Document PSRG-2013-13 presented to the Pacific Scientific Review Group, April 2013. 7 p.

Eddelbuettel, D. and Francois, R. 2011. Rcpp: Seamless R and C++ Integration. – J. Stat. Softw. 40: 1–18.

Kleiber, M. 1975. The fire of life. An introduction to animal energetics. – R.E. Kteiger Publishing Co.

Lockyer, C. 1981. Growth and energy budgets of large baleen whales from the Southern Hemisphere. – Mamm. seas (FAO Fish. Ser. no. 5) 3: 379–487.

Mangel, M. and Clark, C. W. 1988. Dynamic modeling in behavioral ecology. – Princeton Univ. Press.

Monnahan, C. C. et al. 2015. Do ship strikes threaten the recovery of endangered eastern North Pacific blue whales? – Mar. Mammal Sci. 31: 279–297.

Parsons, T. L. 2018. Invasion probabilities, hitting times, and some fluctuation theory for the stochastic logistic process. – J. Math. Biol. 77: 1193–1231.

Pirotta, E. et al. 2018. A dynamic state model of migratory behavior and physiology to assess the consequences of environmental variation and anthropogenic disturbance on marine vertebrates. – Am. Nat. 191: E40–E56.

Potvin, J. et al. 2012. Metabolic expenditures of lunge feeding rorquals across scale: implications for the evolution of filter feeding and the limits to maximum body size. – PLoS One 7: e44854.

R Development Core Team 2016. R: A language and environment for statistical computing. R Foundation for Statistical Computing, Vienna, Austria. ISBN 3-900051-07-0, URL http://www.R-project.org/. in press.

Williams, T. M. 1999. The evolution of cost efficient swimming in marine mammals: limits to energetic optimization. – Phil. Trans. R. Soc. B 354: 193–201.